Chemical Engineering Journal 338 (2018) 636–650

Contents lists available at ScienceDirect

Chemical Engineering Journal

journal homepage: www.elsevier.com/locate/cej

Hydrodynamics of countercurrent bubble column: Experiments and predictions

R. Trivedi, T. Renganathan*, K. Krishnaiah[1]

Department of Chemical Engineering, Indian Institute of Technology Madras, Chennai 600 036, India

HIGHLIGHTS

- Study of hydrodynamics of countercurrent bubble column with a porous distributor.
- Comprehensive flow regime map developed with all four regimes.
- Method developed to predict gas holdup and transition gas velocity semi-empirically.
- Estimated bubble diameter decreases with liquid velocity in homogeneous regime.
- Apparent slip velocity increases with phase velocities in heterogeneous regime.

GRAPHICAL ABSTRACT

Prediction of gas holdup and regime transition points combining two phenomenological models.

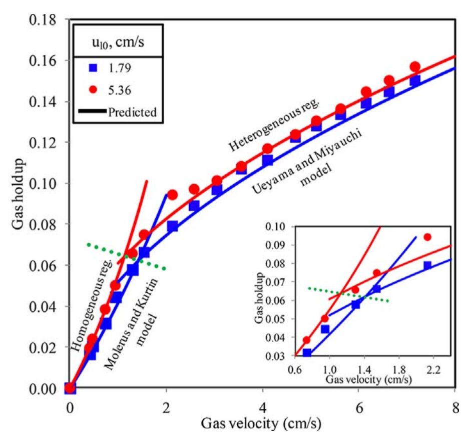

ARTICLE INFO

Keywords:
Bubble column
Countercurrent
Hydrodynamics
Flow regimes
Gas holdup
Apparent slip velocity

ABSTRACT

Experiments were conducted to study the hydrodynamics of a countercurrent bubble column equipped with porous plate distributor. Four flow regimes – purely homogeneous bubbling regime, discrete bubbling regime, helical flow regime and churn-turbulent regime are identified based on the bubble swarm velocity plot. Regime maps are presented showing the effect of liquid velocity on transition gas velocity and gas holdup along all three transition boundaries. The liquid velocity advances the onset of discrete bubbling regime, helical flow regime and churn-turbulent regime. Gas holdup increases with an increase in gas and liquid velocities. A methodology for predicting the gas holdup for both the homogeneous and heterogeneous regimes and the transition gas velocity and holdup is developed by extending existing models for homogeneous and heterogeneous regime. Bubble diameter, the model parameter in homogeneous regime, decreases with an increase in liquid velocity. Apparent slip velocity between gas and liquid phase, the model parameter in heterogeneous regime, increases with both gas and liquid velocity. The method predicts the data of the present work and literature satisfactorily. The effect of gas and liquid velocities on the radial profile of liquid velocity and its properties are simulated using the validated model.

* Corresponding author.
E-mail address: renga@iitm.ac.in (T. Renganathan).
[1] Present address: Indian Institute of Technology Tirupati, Tirupati 517 506, India.

https://doi.org/10.1016/j.cej.2018.01.023
Received 9 August 2017; Received in revised form 3 January 2018; Accepted 4 January 2018
Available online 05 January 2018

Nomenclature

A, B, C	Parameters in the apparent slip velocity correlation Eq. (35)
c	Parameter in Eq. (15)
d_b	diameter of bubble, m
D	diameter of column, m
Fr_g	Gas phase Froude number, dimensionless
g	acceleration due to gravity, m/s^2
H	Height of the column, m
h	pressure head of water, m
$I(\phi)$	Eq. (26)
J_0, J_1	Eqs. (24) and (25)
Mo_l	Liquid phase Morton number, dimensionless
n	Exponent in Eq. (15)
P	Pressure, Pa
$\Delta P/\Delta z$	Pressure gradient
R	Radius of the column, m
r	Radial coordinate, m
r_o/δ	Length ratio, Eq. (2)
Re	Bubble Reynolds number, dimensionless
Re_g	Gas phase Reynolds number, dimensionless
u_{g0},u_{l0}	Superficial phase velocities = $\frac{Volumetric\ flow\ rate}{Column\ cross-sectional\ area}$
u_g,u_l	Interstitial phase velocities, m/s
u_{lc}	Centreline velocity of liquid, m/s
u_{lw}	Liquid velocity at wall, m/s
$u_{l\delta}$	u_l at y = δ, m/s (Eq. (9))
u_s	Apparent slip velocity of bubbles, m/s
$u_{l_{rec}}$	Mean liquid recirculation velocity, m/s
z	Axial coordinate, m

Greek letter

β	Dimensionless bubble diameter, dimensionless
β_0	Dimensionless bubble diameter at batch liquid condition, dimensionless
δ	Thickness of the laminar sublayer, m
ε_c	Centreline gas holdup, dimensionless
ε_g	Average gas holdup, dimensionless
ε_{gr}	Radial gas holdup, dimensionless
ν_t	Turbulent kinematic viscosity, m^2/s
ν	Molecular kinematic viscosity, m^2/s
ρ_l,ρ_g	Phase density, kg/m^3 ξ
τ	Shear stress, kg/ms^2
τ_w	Shear stress at wall, kg/ms^2
ϕ	r/R, Radial coordinate, dimensionless
ϕ^*	Radial coordinate at which flow reverses, dimensionless
μ_g,μ_l	Phase viscosity, kg/m.s
ζ	Dimensionless parameter, Eq. (2)

Abbreviation

AR	Aspect Ratio
CCBC	Continuous Countercurrent Bubble Column
RMS	Root Mean Square

Subscript

g	gas
l	liquid
Exp	Experimental
Pred	Predicted

1. Introduction

Bubble columns in which gas is sparged into a batch of liquid have high heat and mass transfer characteristics and are easy to operate, as there are no moving parts. These multiphase contactors find applications in chemical, biochemical and metallurgical industries [1]. Bubble columns, used for applications such as hydrogenation, fermentation usually have the liquid phase in batch mode. However, applications such as waste-water treatment and ozonation of water involve continuous flow of the liquid phase [2]. Countercurrent flow of liquid has the advantage of high holdup leading to higher mass transport rates [1]. Countercurrent flow of gas and liquid also occurs in three-phase inverse fluidized bed which can be considered as a countercurrent bubble column (CCBC) with suspended solids [3,4].

Experimental studies on bubble column have predominantly been carried out with the liquid phase under batch condition. Relatively few studies have been carried out with continuous flow of liquid. Among these studies with continuous liquid phase flow, fewer studies have been reported on countercurrent flow compared to cocurrent flow bubble columns. A summary of hydrodynamic studies conducted is presented in Table 1. It can be observed that except for the recent comprehensive studies by Besagni and Inzoli [5] and Besagni et al. [6],

Table 1
Summary of literature on hydrodynamics of CCBC.

Authors	D; H; AR (m)	Gas sparger	u_{g0} (cm/s)	u_{l0} (cm/s)	Hydrodynamic aspects studied		
					Flow regimes	Gas holdup	Bubble size distribution
Eissa and Schügerl [31]	0.159; 3.9; 24.5	Perforated plate	0–6	0.35, 0.7, 1.05	✗	✓	✗
Todt et al. [52]	0.14; 3.8; 27.1	Perforated plate	0.67–10.67	0.7–2.38	✗	✓	✗
Otake et al. [7]	0.05; 1.5; 30	Single and multi-nozzles	0.7–8.24	0–14	✗	✓	✗
Uchida et al. [8]; Seno et al. [9]	0.046; 1.36; 29.5	Single nozzle and porous glass ball filter	0–4	0–10	✓	✓	✗
Ityokumbul et al. [22]	0.06; 1.06; 17.7	Porous plate	0–4	0–0.76	✓	✓	✗
Roustan et al. [10]	0.15; 2.5; 16.7	Porous distributor	0.19–2.08	0.44–2.08	✗	✓	✓
Hidaka et al. [11]	0.07; 4.25; 60.7 & 0.15; 2.6; 18	Spiral copper tube	2–30	0–15	✗	✓	✗
Bin et al. [15]	0.15; 5.5; 36.7	Porous gas distributor	0.47–1.88	0.16–0.71	✗	✓	✗
Son et al. [16]	0.152; 3.5; 23	Pipe distributor	1–3.5	0–3	✗	✓	✓
Jin et al. [12]	0.16; 2.5; 15.6	Perforated plate	2–25	0–1.12	✓	✓	✗
Shah et al. [14]	0.29; 2; 6.9	Perforated plate	2–11	0.05–0.2	✗	✓	✗
Hernandez-Alvarado et al. [13]	0.1; 1.6; 16	Not available	4.6–20.6	2.1–20	✗	✓	✗
Besagni & Inzoli [5]; Besagni et al. [6]	0.24; 5.3; 22.1	Spider sparger	0.4–20	0–9.2	✓	✓	✓

limited studies have been reported on CCBC over the years. The main aspects studied by these authors included flow regimes, and effect of gas and liquid velocities on gas holdup.

Flow regimes in CCBC have been studied by very few authors. The nature of flow regimes identified in CCBC varies among different studies. Otake et al. [7] observed uniform bubbling flow, transition flow and churn-turbulent flow regime. In addition to bubble flow and churn-turbulent flow regimes, Uchida et al. [8] and Seno et al. [9] identified a bubble-downflow regime at low gas velocity and high liquid velocity conditions wherein bubbles start flowing downward with the liquid to the bottom. Three flow regimes viz. homogeneous, transition and heterogeneous regimes were identified by Besagni and Inzoli [5] and Besagni et al. [6]. The effect of liquid velocity on the transition velocities has been discussed only by Besagni and Inzoli [5]. In general, the flow regime data from the literature by these authors show that increase in liquid velocity advances the onset of the heterogeneous regime.

The effect of gas velocity on the gas holdup is similar to that of bubble column with batch liquid. All the authors have studied the effect of liquid velocity on gas holdup and show an increase in gas holdup with increase in liquid velocity. However the degree of effect differs between the authors. Roustan et al. [10] observed almost insignificant effect of liquid velocity on gas holdup for low range of liquid velocities. The data of Hidaka et al. [11] and Besagni and Inzoli [5] indicates that the effect of liquid velocity on gas holdup diminishes with increase in gas velocity. Similar conclusions can be drawn from the radial distribution of gas holdup (centreline gas holdup) measured by Jin et al. [12]. Recently, the radial profile of gas holdup was also measured by Hernandez-Alvarado et al. [13] using different measurement techniques. These authors concluded that the downward liquid flow in CCBC causes higher gas holdup at the centre compared to other modes of bubble column. Contrary to the above studies Shah et al. [14] have shown a decrease in gas holdup with increase in liquid velocity.

Similar to batch bubble columns, different gas distributors have also been used in CCBCs. In addition to steady and uniform gas distribution, an additional criterion to be considered in the selection of distributor for CCBC is, it should allow the liquid flowing downwards to flow freely out of the column, without disturbing the flow inside the column. Hence, gas distributors have been used in CCBC paying due attention to this criterion. The different types of gas distributors used in CCBC are shown in Table 1. Most of the studies in literature have used some form

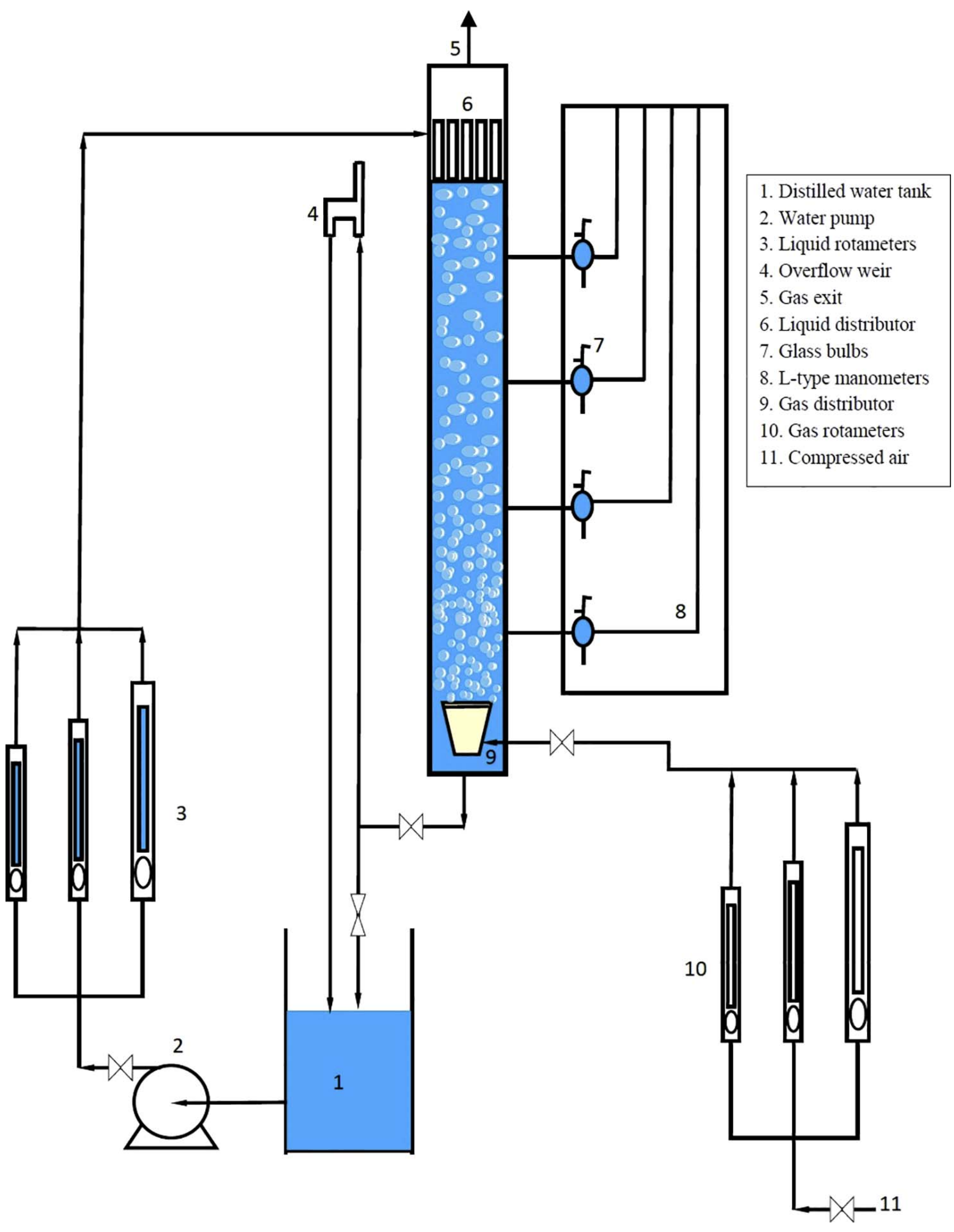

Fig. 1. Schematic of the experimental setup.

of orifice type distributors (perforated plate, spider sparger, spiral tube) or nozzle type distributors.

Some attempts have been made to predict the hydrodynamics of CCBC. Besagni et al. [6] proposed an empirical relation to predict the regime transition velocity. Empirical correlation was proposed for average gas holdup by Roustan et al. [10], Bin et al. [15] and Son et al. [16] in the homogeneous regime, by Uchida et al. [8], Seno et al. [9] and Shah et al. [14] in the heterogeneous regime and by Otake et al. [7] and Besagni et al. [6] in both the regimes. Jin et al. [12] proposed an empirical correlation for the centreline gas holdup. Among all these, only the correlations proposed by Otake et al. [7], Uchida et al. [8], Seno et al. [9], Jin et al. [12] and Besagni et al. [6], correctly approach the limiting condition of batch liquid. Hidaka et al. [11] used the simplified form of the recirculation model of Ueyama and Miyauchi [17] and predicted gas holdup in the heterogeneous regime by fitting turbulent viscosity and apparent slip velocity applicable for their data alone.

The above survey of the literature on CCBC reveals the following: (1) most of the experimental studies were conducted using only orifice or nozzle type distributors or with porous distributors for very narrow range of phase velocities (2) comprehensive studies on flow regime maps covering all regimes are limited (3) attempts to predict the hydrodynamics are either empirical or limited to a particular regime. Compared to orifice or nozzle type distributors, porous plate distributors result in bubbles of smaller sizes that aid higher mass transfer. Consequently, the objectives of the present work are (1) to study the hydrodynamics of CCBC using porous plate distributor over a wide range of phase velocities specifically focussing on the detailed regime map covering all the four regimes and (2) develop a methodology to semi-empirically predict the gas holdup of the present study and literature in all the regimes including the regime transition points.

2. Experimental details

A schematic diagram of the experimental setup of the CCBC is shown in Fig. 1. The test section of CCBC is made of multiple sections of acrylic columns. The test section has an internal diameter of 89 mm and a height of 1.85 m. A heat exchanger type liquid distributor is used at the top of the column. Liquid is distributed though 2 mm holes at the bottom of the shell side of the distributor. Gas escapes through 11 mm tubes arranged axially inside the shell. The gas distributor constituted an 8 mm thick sintered glass disc made up of Borosil Grade 2 porous glass dust, with pore size 40–90 µm, fixed at the top of a PVC shower facing upward. The outer diameter of the gas distributor was 65 mm so as to allow the water to leave the column through the annular area between the gas distributor and column (I.D. 89 mm).

In the present work, distilled water and air were used as liquid and gas phase respectively, at ambient temperature and pressure. Water was pumped from the storage tank to the liquid distributor through calibrated set of rotameters. Water distributed at the top of the column exited the bottom through annular area between gas distributor and column and was recirculated back to the storage tank through an overflow weir. This overflow weir was used to maintain constant water level inside the column. Compressed air was introduced from the bottom of the column through a set of calibrated gas rotameters. This compressed air was allowed to enter the column through porous gas distributor with uniform distribution throughout and escaped through the tubes in the liquid distributor at the top. Static pressure drop across the test section was measured using L-type manometers. Glass bulbs were used between the pressure tappings and the L-tubes. These glass bulbs helped in avoiding air bubbles entering the manometers and large oscillations in the liquid head. The test section of the column was graduated using a graph sheet to enable visual measurement of height of the gas-liquid dispersion.

Experiments were conducted at ambient conditions by setting different flowrates of liquid and by varying the gas flowrate. Once steady state was attained, the pressure drop across the column was noted to calculate the average gas holdup in the column according to the following relation

$$\varepsilon_g = 1 + \frac{1}{\rho_l g}\frac{\Delta P}{\Delta z} \tag{1}$$

The gas holdup calculated from pressure drop measurement was found to be in good agreement with that obtained by the level swell method. The flow regime that prevailed in the column for each combination of gas and liquid flowrates was also carefully observed by visual observation. Experiments were carried out over the following range of superficial phase velocities: gas velocities from 0.23 to 7.17 cm/s and liquid velocity from 0 to 7.14 cm/s.

3. Results and discussion

The experimental results obtained on flow regimes and gas holdup in the countercurrent bubble column is discussed in this section, qualitatively comparing them with the literature data.

3.1. Flow regimes

Different methods have been proposed in the literature for identification of flow regimes in bubble columns [18]. Among these, the swarm velocity method of Zuber and Findlay [19] and drift flux method of Wallis [20] use the data on average gas holdup in the column vs. gas velocity. Compared to the Wallis's [20] drift flux variation, the swarm velocity variation is more sensitive to flow regime changes. So the swarm velocity method is capable of showing different regime transitions more clearly than the Wallis's [20] drift flux method. While the drift flux method can show only one regime transition, swarm velocity method can show multiple regime transitions. Hence the swarm velocity method is used in the present work to identify regime transition velocities.

Fig. 2 shows the variation of gas hold up with gas velocity for a constant liquid velocity. The swarm velocity $\left(u_{swarm} = \frac{u_{g0}}{\varepsilon_g}\right)$ which represents the velocity of the bubbles in the swarm is also shown in the same graph as a function of gas velocity. Four flow regimes can be identified using the swarm velocity plot. This identification is based on the observation that, the bubble swarm velocity plotted against superficial gas velocity shows change of slope for every change of regime. In Regime I, the bubble swarm velocity decreases with gas velocity due to the retarding effect of downflowing liquid carried by bubbles [21]. In Regime II the bubble swarm velocity can be approximated to be almost constant. It can be noted that the swarm velocity in Regime II is not

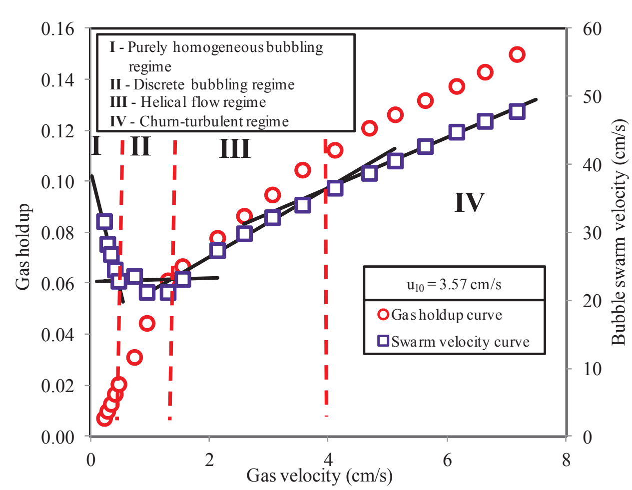

Fig. 2. Flow regimes in countercurrent bubble column.

strictly a constant, but it can be approximated to a constant in line with the simplification conventionally adopted in the literature for identification of regime transitions. The variation in the bubble swarm velocity in Regime II can also be observed in the data reported by other authors [5,22]. As discussed by Ruzicka et al. [21], this region is marked by the competition between the retarding effect of the downflowing liquid carried by bubbles and the enhancement effect by liquid recirculations on the rise velocity of the bubbles. This competition could be the reason for the minor variation of swarm velocity in Region II. In Regimes III and IV the bubble swarm velocity increases due to the enhancement caused by the liquid recirculations [21]. The relatively lower increase in the swarm velocity in Regime IV compared to Regime III may be because of bubble breakage in Regime IV.

In each regime, the swarm velocity can be approximated by a straight line and the points of intersection of these lines give the regime transition velocities. Straight line was fitted to the swarm velocity vs. gas velocity data in the respective regimes and the transition gas velocity was calculated by simultaneous solution of the two straight line equations. The different flow regimes identified based on the swarm velocity plot matched well with the visual observations on the hydrodynamic changes in the different regimes. In the following are given the detailed qualitative explanations for the four flow regimes observed.

The Regime I occurs at very low gas velocities. Herein, the gas bubbles are nearly spherical without any distortion, uniformly sized, homogeneously spaced, and rise up virtually vertically, undisturbed in the continuous liquid phase almost like a swarm of bubbles in plug flow. This regime is described as the purely homogeneous bubbling regime. This regime has been identified by Ityokumbul et al. [22] as chain bubbling regime. This regime can also be observed from the data of Besagni and Inzoli [5]. As the gas velocity increases, Regime II appears. Herein, the homogeneous bubbles of the previous regime are slightly deformed to ellipsoids and are no longer uniformly spaced. In this regime, with increasing gas velocity, increase in bubble-bubble interaction, in the uprising swarm becomes quite apparent. This regime is termed as the discrete bubbling. These two regimes together have been termed as uniform bubbling flow regime [7] or bubble flow regime [8,9] or homogeneous regime [5,6].

Further increase in the gas velocity causes the distance between the neighbouring bubbles to decrease, increasing collisions of the bubbles resulting in their coalescence. These coalesced, fast rising, distorted bubbles move helically in the central core of the column. Such large helical movement causes gross circulations in the liquid phase. Hence this regime is named as helical flow regime (Regime III). A similar observation was made by Chen et al. [23] and Cui [24] in semibatch bubble columns and was named as vortical-spiral flow. Regime III has also been identified by Otake et al. [7], Besagni and Inzoli [5] and Besagni et al. [6] in CCBC and termed as transition flow regime.

The large scale recirculations in Regime III, in turn triggered churning and hence the onset of the next churn-turbulent flow regime (Regime IV). With further increase in the gas velocity, gross circulations increased resulting in higher liquid phase turbulence. Such high turbulence causes breakage of the coalesced bubbles into bubbles of irregular shape. Regime IV has been identified by most of the authors, yet the boundary between Regimes III and IV are discussed by very few authors (e.g. Nedeltchev [25], in semibatch bubble columns and Besagni et al. [6], in CCBC).

The bubble swarm velocity method to identify the flow regimes has been employed by several other authors in the literature [26–30,5,6]. However the number of regimes identified differs between the authors based on the range of gas velocities as shown in Table 2. It can be noted that the present study is more comprehensive than the other studies in the literature in identifying all the four regimes. While Regimes II and III have been identified in most of the studies, very few studies have identified Regimes I and IV.

3.2. Flow regime map

The flow regime transition gas velocities identified above for a particular liquid velocity, can be obtained for other liquid velocities also. The transition gas velocities for each liquid velocity are identified based on the swarm velocity plot for that particular liquid velocity. The bubble swarm velocity plot for different liquid velocities is shown in Fig. 3. The three regime transition boundaries/gas velocities (between the four regimes) identified using the swarm velocity method is shown in Fig. 4(a) as a function of liquid velocity. In general, all the transition gas velocities decrease with increase in liquid velocity in the CCBC. Increasing the liquid velocity brings the bubbles closer which can cause more bubble-bubble interaction leading to an early transition from Regime I to Regime II. With increase in liquid velocity, the number density of the bubbles increases thereby increasing the probability of coalescence between the bubbles for relatively higher gas velocities. This results in early transition from Regime II to Regime III. The regime transition between Regimes III and IV occurs at high gas velocities. Under conditions of such high gas velocities, increasing the liquid velocity causes more breakage of the bubbles. This might be the reason for an early onset of the churn-turbulent flow regime which is characterised by bubble breakage.

Fig. 4(b) shows the variation of the gas holdup with liquid velocity along the three transition regime boundaries. The gas holdup at the transition velocities were obtained from the experimental ε_g vs. u_{g0} data by interpolation for the calculated transition velocities. In general it can be seen that the gas holdup increases along all the three regime transition boundaries. This increase in holdup is also responsible for early occurrence of different flow regimes, with increase in liquid velocity. Comparing Fig. 4(a) and (b) it can be seen that, the liquid velocity has a clear decreasing effect in the case of transition gas velocity. However, in the case of transition gas holdup, increase in gas holdup with liquid velocity can be seen on an average with small variations. Such increasing trend with small variations can also be observed in the transition gas holdup reported by Besagni and Inzoli [5] for CCBC. This could be because of the following reason: With increase in liquid velocity, the gas holdup increases in the countercurrent operation. However, with increase in liquid velocity, the transition gas velocity decreases which can cause the gas holdup to decrease. Hence the net variation of the gas holdup along the regime transition boundary is determined by the balance between the two opposite effects, one due to increasing liquid velocity and the other due to decreasing transition gas velocity.

In the literature on CCBC, the effect of liquid velocity on the transition gas velocity and gas holdup has been observed by Besagni and Inzoli [5] only. The authors studied the effect of liquid velocity on Regime II/III transition boundary only. The effect of liquid velocity observed in the present study for Regime II/III transition boundary is in line with the observations of Besagni and Inzoli [5]. It should be noted that to the best of our knowledge there are no other studies in the literature on CCBC that report effect of liquid velocity along other

Table 2
Flow regimes identified in different studies.

Authors	Mode of operation	Regimes identified			
		I	II	III	IV
Krishna et al. [26]	Batch BC	✗	✓	✓	✗
Gourich et al. [28]	Batch BC	✗	✓	✓	✗
Ribeiro and Mewes [29]	Batch BC	✗	✓	✓	✗
Letzel et al. [30]	Batch BC	✗	✓	✓	✗
Ityokumbul et al. [22]	CCBC	✓	✓	✓	✗
Hyndman et al. [27]	Batch BC	✗	✓	✓	✓
Besagni and Inzoli [5]; Besagni et al. [6]	CCBC	✗	✓	✓	✓
Present Study	CCBC	✓	✓	✓	✓

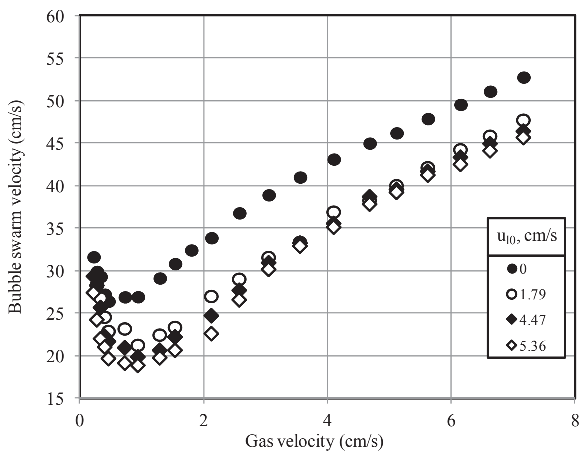

Fig. 3. Swarm velocity plots for different liquid velocities.

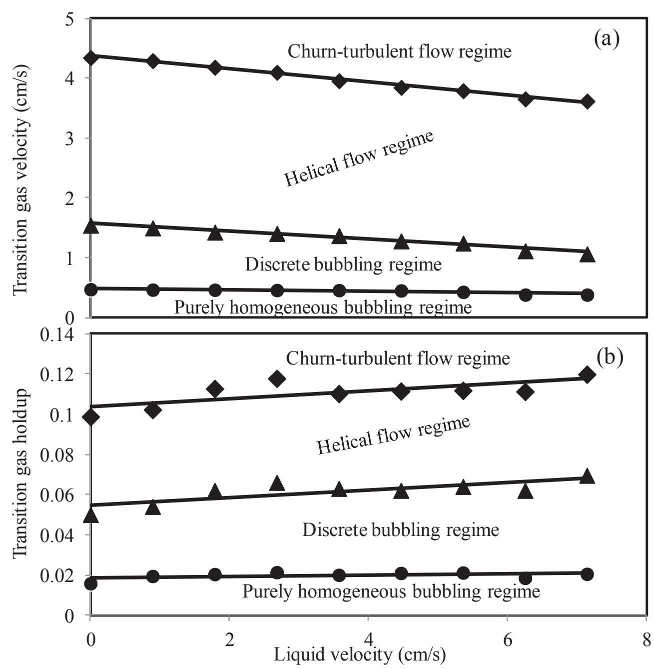

Fig. 4. Flow regime map in CCBC (a) transition gas velocities (b) transition gas holdup.

transition boundaries.

3.3. Effect of gas velocity on gas holdup

The effect of gas velocity on gas holdup is shown in Fig. 5 for different liquid velocities along with regime transition boundaries drawn based on Fig. 4. The nature of the gas holdup curve for the CCBC is almost similar to that for semibatch and cocurrent bubble columns. The trend observed in the present work for CCBC is similar to those reported in the literature (e.g. Eissa & Schugerl [31], Bin et al. [15], Jin et al. [12], Besagni and Inzoli [5], Besagni et al. [6]). Increase in gas velocity causes the gas holdup to increase throughout all the four regimes because of increase in bubble population in the column. For the lower ranges of gas velocities, in the purely homogeneous and discrete bubbling regimes (I and II), the gas holdup vs. gas velocity is convex in shape implying that the gas holdup increases at higher rate with increase in gas velocity. This can be explained by the retarding effect of liquid carried by the rising bubbles [21]. With increase in liquid velocity, the gas holdup curve become less convex because, with increasing velocity of liquid flowing downwards, the contribution of the retarding effect of liquid carried by rising bubbles reduces. Further, for any liquid velocity, near the end of the discrete bubbling regime (II), the gas holdup increases with superficial gas velocity at a higher rate almost approaching linear variation probably due to the onset of the bubble coalescence and the accompanying enhancement effect [21].

In the helical flow and churn turbulent flow regimes (III and IV), the coalescence of gas bubbles is predominant causing gross circulations in the liquid phase. The upward motion of the circulating liquid aids the rise of bubbles and due to this enhancement effect, the gas holdup plot is concave indicating that the gas holdup increases with gas velocity at a lower rate [21]. It can also be observed that with increase in liquid velocity, the gas holdup shows a small local maximum with gas velocity. Such a maximum is also observed in the data of Besagni and Inzoli [5] for higher liquid velocities. This can be attributed to the sudden escape of coalesced bubbles from the column leading to local decrease in gas holdup. In a batch bubble column, such a decrease is observed when a gas distributor with perforations less than 1 mm is used or liquid with surface active agents is used [32]. Based on the present study in CCBC, it is clear that high liquid velocities in the countercurrent direction can also give rise to such a trend.

3.4. Effect of liquid velocity of gas holdup

Fig. 6 shows the effect of liquid velocity on gas holdup in the CCBC along with regime transition boundaries. In general, the gas holdup increases with increase in liquid velocity. It can be seen that the gas holdup increases more at low liquid velocities especially near batch liquid condition, than at high liquid velocities. Increase in liquid velocity, reduces the rise velocity of the bubbles, leading to an increase in their gas holdup due to increase in their residence time inside the column. Increase in liquid velocity can also cause breakage of bubbles which can also contribute to increased gas holdup. In Regimes III and IV, coalescence between bubbles may increase with liquid velocity which can cause reduction in gas holdup. Thus the variation of gas holdup with liquid velocity appears to be determined by these three competing mechanisms, increased residence time of bubbles and bubble breakage causing increase in gas holdup and bubble coalescence causing decrease in gas holdup.

Effect of liquid velocity on gas holdup in CCBC has been studied in the literature by different authors. Fig. 7 shows the effect of superficial liquid velocity on gas holdup based on the gas holdup data measured by Hidaka et al. [11] and Besagni and Inzoli [5]. The liquid velocity is seen to increase the gas holdup in these studies as well. In the case of Besagni and Inzoli [5] and Hidaka et al. [11], the effect of liquid velocity decreases with increase in gas velocity. At high gas velocities the gas induced liquid recirculations are very high which reduce the effect of

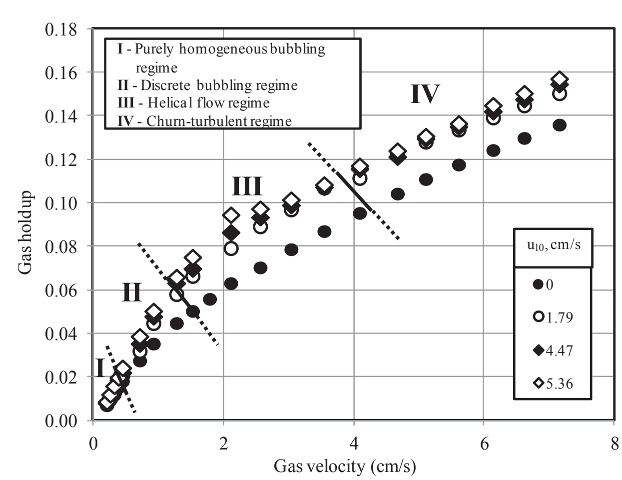

Fig. 5. Effect of gas velocity on gas holdup.

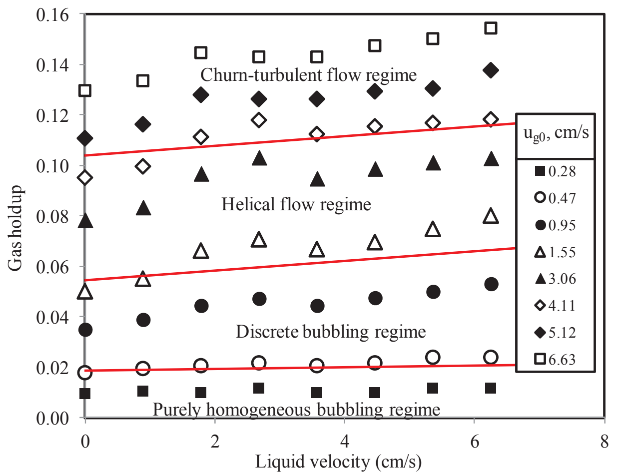

Fig. 6. Effect of liquid velocity on gas holdup in the present study (Lines represent regime boundaries).

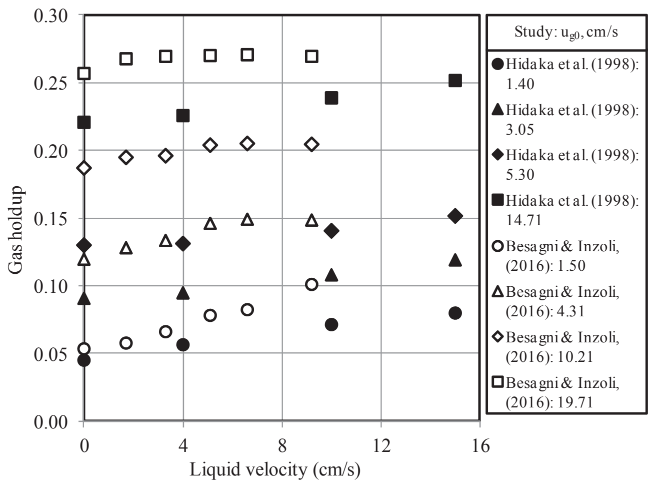

Fig. 7. Effect of liquid velocity on gas holdup (from literature).

external liquid flow. This effect is not observed in the present study probably due to the lower ranges of gas velocities studied.

4. Prediction of hydrodynamic variables

In this section, a methodology is developed to predict the hydrodynamic variables measured in the CCBC in the present study and literature. Specifically, the variation of the gas holdup with the phase velocities and regime transition velocity and gas holdup are predicted. For this purpose, only two regimes are distinguished. Regimes I and II are termed together as homogeneous regime and Regimes III and IV are termed together as heterogeneous regime. These two regimes are modelled separately.

4.1. Homogeneous regime

The data on ε_g vs. u_g in the present study follows a convex trend at low gas velocities due to the occurrence of a homogeneous regime. Most of the empirical correlations proposed for bubble columns are applicable for the purely heterogeneous case since the correlations show a concave trend even at very low gas velocities. The correlation proposed by Besagni et al. [6] recently for CCBC also does not show a convex trend at low gas velocities. The models/empirical equations which show a convex trend in the homogeneous regime are limited. The correlation of Richardson and Zaki [33] in terms of slip velocity and of Garnier et al. [34] depicts a convex trend in the homogeneous regime; however these are purely empirical. The semi-empirical model proposed by Molerus and Kurtin [35], the simple physical model of Ruzicka et al. [21], and methodology of Nedeltchev and Schumpe [36] also shows a convex trend. The method of Nedeltchev and Schumpe, [36] depends on the empirical correlation proposed by Wilkinson et al. [37] for small bubble diameter and is limited to semibatch bubble column. Similar to the Richardson and Zaki [33] equation, the model of Ruzicka et al. [21] has two empirical parameters viz. bubble terminal velocity and bubble drift coefficient. The model of Molerus and Kurtin [35] has one parameter viz. bubble diameter, is phenomenologically more detailed and much directly related to the bubble swarm drag coefficient. Hence the semi-empirical model proposed by Molerus and Kurtin [35] is chosen to predict the homogeneous ε_g vs. u_g data.

Molerus [38] proposed a cell model to predict the bed expansion in a liquid-solid fluidized bed. The model equation is equivalent to a relation for drag coefficient between the solid and liquid. Based on experimental data in liquid-solid fluidized bed the constants in the equation were fitted. The same equation was applied by Molerus and Kurtin [35] to describe the hydrodynamics (gas holdup, bubble size and transition velocity) of bubble column in the homogeneous regime. The constants in the equation were refitted using more experimental data in the literature by Molerus [39]. This model as applied to a CCBC is given as

$$\beta^3 = 18\left\{1 + 0.341\left[\frac{r_0}{\delta} + \frac{1}{2}\left(\frac{r_0}{\delta}\right)^2\right]\right\}Re + 3\left[1 + 0.07\left(\frac{r_0}{\delta}\right)^{1.5}\right]Re^{1.5} + \left[0.3 + \frac{0.68}{Re^{0.1}}\left(\frac{r_0}{\delta}\right)\right]Re^2$$
$$\text{where, } \frac{r_0}{\delta} = \frac{1}{\left(\frac{\xi}{\sqrt[3]{\varepsilon_g}}\right) - 1} \text{ with } \xi = 0.9 \tag{2}$$

where β is the dimensionless bubble diameter defined as

$$\beta^3 \equiv \left(\frac{\rho_l - \rho_g}{\rho_l}\right)\left(\frac{d_b^3 g}{\nu^2}\right) \tag{3}$$

and Re is the Reynolds number defined as

$$Re = \left[\left(\frac{u_{g0}}{\varepsilon_g} + \frac{|u_{l0}|}{1-\varepsilon_g}\right)d_b\right]\nu^{-1} \tag{4}$$

In the case of liquid-solid fluidized bed, the particle diameter is known and hence the equation can be used to predict bed voidage. But in the case of bubble column, the bubble diameter is not known apriori and hence cannot be used directly to predict the gas holdup. However, the equation can be used to estimate the bubble diameter from a data of gas holdup vs. gas velocity. Molerus and Kurtin [35] applied this model to estimate the bubble diameter in bubble columns with batch liquid which compared with the experimentally measured bubble diameter satisfactorily. The above model is used to estimate the diameter of bubble in countercurrent bubble column based on experimental gas holdup data measured in the present work and Besagni and Inzoli [5]. For each liquid velocity, the dimensionless bubble diameter, β is fitted such that the RMS error between the experimental and predicted gas holdups is minimized.

The dimensionless bubble diameter β fitted for each liquid velocity is normalized with the dimensionless bubble diameter β_0 fitted for batch liquid condition. The variation of the normalized bubble diameter with liquid velocity for the present study together with Besagni & Inzoli [5] is shown in Fig. 8. It is seen that the normalized bubble diameter decreases with liquid velocity for both the data of the present work and Besagni & Inzoli [5]. The decrease in bubble diameter can be attributed to the breakage caused by the increased turbulence with increase in liquid velocity [5]. Few preliminary experiments were done with the CCBC setup at low gas velocities to verify this trend. Compared to the batch liquid condition, the mean (calculated from bubble size

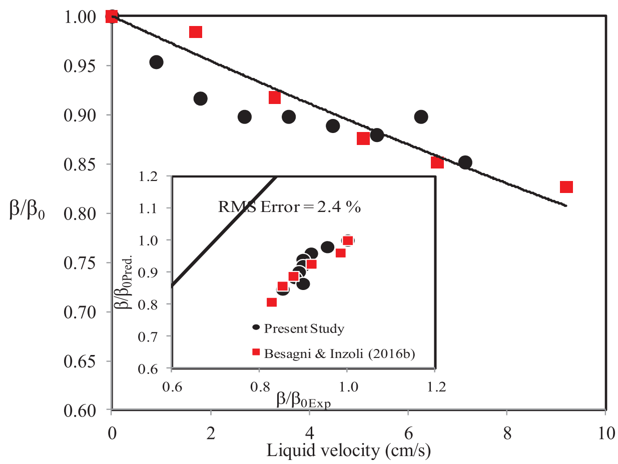

Fig. 8. Variation of dimensionless bubble diameter with liquid velocity.

distribution) bubble diameter decreased for a high liquid velocity. Besagni and Inzoli [5] have experimentally measured the bubble diameter for different gas velocities under batch liquid condition and at a liquid velocity of 6.6 cm/s in countercurrent mode. The bubble diameter averaged over the gas velocities showed an increase under counterflow condition compared to batch liquid condition. The reason for this increase in bubble diameter is not clear from their discussion. The average bubble diameter at the distributor has been shown to increase with liquid velocity under counterflow condition due to delayed release from the distributor by Takahashi et al. [40]. However to our best knowledge there are no other studies which give the effect of liquid velocity on average bubble diameter in the column under countercurrent flow condition. Given the limited data (for only one countercurrent liquid velocity) reported by Besagni and Inzoli [5] and in the absence of other data in the literature, more studies are required to confirm the correct trend.

The effect of liquid velocity on the dimensionless bubble diameter can be expressed by the following empirical equation fitted using the experimental data

$$\frac{\beta}{\beta_0} = \exp(-2.33u_{l0});\ \textit{where}\ u_{l0}\ \text{in m/s} \tag{5}$$

with $\beta_0 = 108$ and 121 for the present study and Besagni and Inzoli [5] respectively. It can be noted that the above equation ensures that in the limit of $u_{l0} = 0$ (batch liquid condition), β correctly tends to β_0. This equation predicts the experimental normalized bubble diameters with an RMS error of 2.4% as shown in the inset of Fig. 8.

Using the β predicted from Eq. (5), the Molerus and Kurtin [35] model is used to predict the gas holdup in the homogeneous regime. Fig. 9(a) and (b) show the variation of gas holdup with gas velocity in the homogeneous regime for different liquid velocities as predicted by the Molerus and Kurtin [35] model and compares with the experimental data for the present study and Besagni & Inzoli [5] respectively. It can be seen that the convex nature of the experimental data in both the studies is correctly captured by the predicted lines. Fig. 10 shows the parity plot between the experimental and predicted gas holdups in the homogeneous regime for both the studies with an RMS error of 10.3%.

4.2. Heterogeneous regime

The heterogeneous regime is relatively more complex to model due to the presence of large and small bubbles and the resulting liquid recirculations. Modelling work on fluid dynamics in the heterogeneous regime has been classified into three phases based on chronological development [41]. While Phase I models did not consider the momentum transfer due to turbulence, Phase II and III models included the effect of turbulence through simple and detailed closure models for eddy viscosity respectively. Phase II models are a good compromise between simple Phase I models and computationally intensive Phase III models. In the present work, one of the pioneering Phase II models proposed by Ueyama and Miyauchi [17] is extended to predict the gas holdup in the heterogeneous regime.

4.2.1. Model equations and analytical solution

The liquid recirculation model for predicting the liquid velocity profile in a bubble column operating in the heterogeneous regime with batch and continuous liquid was developed by Ueyama and Miyauchi [17]. This model has been extended in the present work to predict the hydrodynamic characteristics viz. gas holdup and liquid velocity profile of the countercurrent bubble column. In this section the basic equations are presented for the extended model. The basic conservations equations include the momentum balance for the liquid phase and mass balance for the liquid and gas phase.

A typical radial profile of the axial liquid velocity in a CCBC is shown in Fig. 11. The liquid flows upward in the centre of the column, becomes zero at an intermediate radial position and then flows downward near the wall. The flow is turbulent over the entire cross-section except in the downflow region near the wall where it is laminar. The velocity shown is the time-averaged mean velocity. The z-momentum balance which governs the velocity profile is

$$-\frac{1}{r}\frac{d}{dr}(r\tau) = \frac{dP}{dz} + (1-\varepsilon_{gr})\rho_l g \tag{6}$$

The shear stress is related to the velocity gradient by the following equation

$$\tau = -(\nu_t)\rho_l\left(\frac{du_l}{dr}\right) \tag{7}$$

This equation assumes that the molecular viscosity is much smaller than the turbulent viscosity, an assumption that is valid over the entire column except very close to wall where viscous effects are significant. Two boundary conditions are required to solve Eq. (6) for the velocity.

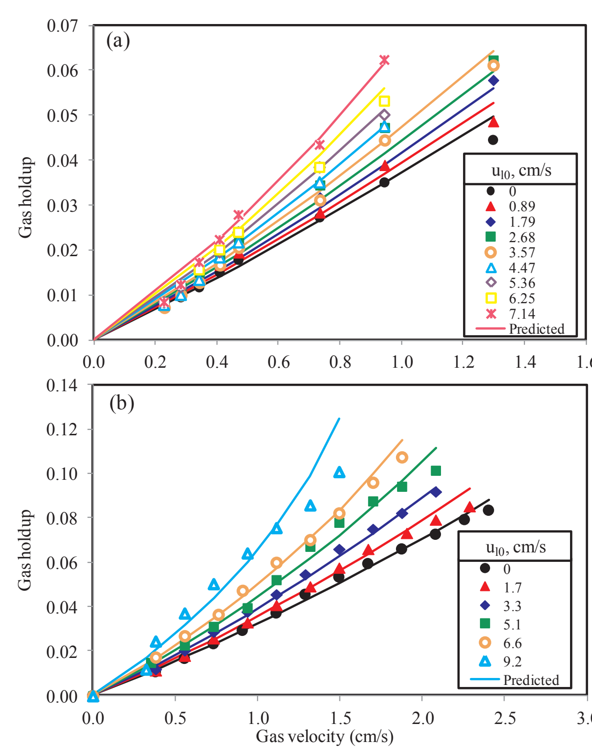

Fig. 9. Prediction of gas holdup in homogeneous regime using model: effect of phase velocities (a) Present data (b) Besagni and Inzoli (2016).

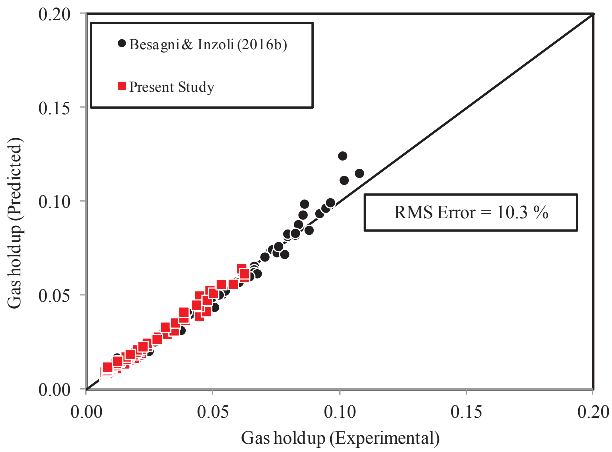

Fig. 10. Comparison of experimental and predicted gas holdup in homogeneous regime.

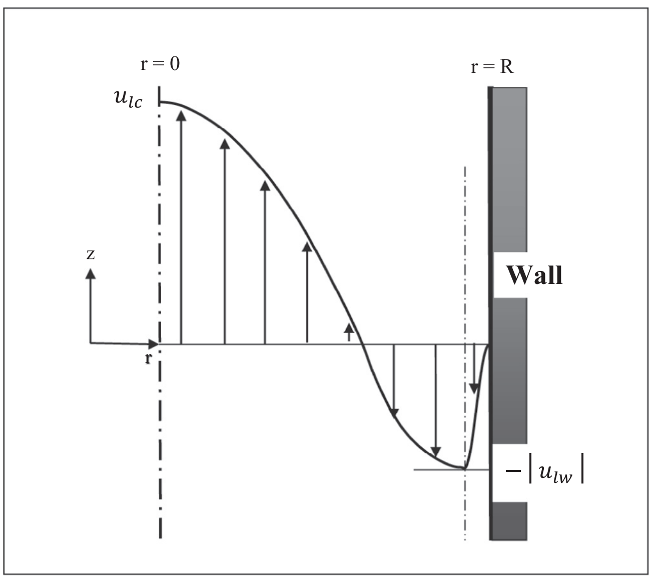

Fig. 11. Typical radial profile of liquid velocity.

The symmetry boundary condition at the centre is given by

$$\frac{du_l}{dr} = 0 \ at \ r = 0 \tag{8}$$

The laminar sublayer near the wall is of very small thickness. Hence the velocity at the wall can be approximated to be the velocity at the intersection of the turbulent core and laminar sublayer. This velocity is given by

$$u_{l\delta} = -11.63\sqrt{\frac{|\tau_w|}{\rho_l}} \tag{9}$$

Hence the boundary condition at the wall is

$$u_{lw} = u_{l\delta} = -11.63\sqrt{\frac{|\tau_w|}{\rho_l}} \ at \ r = R \tag{10}$$

Eq. (6) is solved by following the analytical solution methodology used by Ueyama and Miyauchi [17]. To eliminate the pressure gradient in Eq. (6), it is integrated from $r = 0$ to R to get

$$-\frac{dP}{dz} = \left(\frac{2}{R}\right)\tau_w + (1-\varepsilon_g)\rho_l g \tag{11}$$

The radially-averaged gas holdup ε_g in the above equation is defined as

$$\varepsilon_g = \int_0^R 2\pi r \ \varepsilon_{gr} \, dr/\pi R^2 \tag{12}$$

Eliminating the pressure gradient in Eq. (6) using Eq. (11) and using Eq. (7) for the shear stress, the momentum balance becomes

$$-\frac{1}{r}\frac{d}{dr}\left(\nu_t r \frac{du_l}{dr}\right) = \frac{2}{R\rho_l}\tau_w - (\varepsilon_g - \varepsilon_{gr})g \tag{13}$$

Integration of Eq. (13) requires the radial variation of local gas holdup and turbulent viscosity. The latter is assumed to be independent of the radial position following Ueyama and Miyauchi [17] model. For the radial variation of the gas holdup, Ueyama and Miyauchi [17] assumed the following radial profile

$$\frac{\varepsilon_{gr}}{\varepsilon_g} = \left[\frac{n+2}{n}\right](1-\phi^n) \text{ where } \phi = r/R \tag{14}$$

The gas holdup at the wall is considered to be zero in the above equation. However, non-zero values of gas holdup have been observed in bubble columns with batch liquid [5,42]. To account for this non-zero gas holdup at the wall, Kato et al. [43] proposed the following radial profile

$$\varepsilon_{gr} = \varepsilon_g\left(\frac{n+2}{n+2-2c}\right)\left[1-c\left(\frac{r}{R}\right)^n\right] \tag{15}$$

In the above equation, $c = 1$ corresponds to the case of zero gas holdup at the wall and Eq. (15) simplifies to Eq. (14). In the present work, to allow for non-zero gas holdup at the wall, Eq. (15) is employed for the radial profile.

The value n in the radial profile equation indicates the sharpness of the gas holdup profile, lower the n, sharper the profile. In the work of Ueyama and Miyauchi [17], n was assumed to be a constant ($n = 2$), independent of gas velocity and was found to describe the radial profile of many authors. However, Luo and Svendsen [44], based on experimental evidence, took a value of 8 for n, indicating a much more flatter profile. Similarly a staircase type of gas holdup profile approximating a flat radial gas holdup profile was assumed in the work of Burns and Rice [45]. Hence a wide range of n has been experimentally observed and assumed in the models for heterogeneous regime. Further n can vary with gas velocity, column diameter and other physical properties. To account for this variation of n, Wu et al. [46] proposed the following correlation for n.

$$n = 2.188 \times 10^3 Re_g^{-0.598} Fr_g^{0.146} Mo_l^{-0.004} \tag{16}$$

The same authors also proposed a correlation for c as

$$c = 4.32 \times 10^{-2} Re_g^{0.2492} \tag{17}$$

In the above equations, the dimensionless numbers are defined as

$$Re_g = \frac{D u_{g0}(\rho_l-\rho_g)}{\mu_l} \tag{17a}$$

$$Mo_l = \frac{g\mu_l^4}{(\rho_l-\rho_g)\sigma_l^3} \tag{17b}$$

$$Fr_g = \frac{u_{g0}^2}{gD} \tag{17c}$$

In the present work, the above equations have been used for n and c in the radial profile Eq. (15). Since no experimental data is available on liquid velocity profiles in CCBC, n and c are assumed to be independent of superficial liquid velocity in the present work.

Solving the momentum balance Eq. (13) along with radial profile equation for gas holdup, Eq. (15), the boundary conditions Eq. (8) and Eq. (10), the radial profile of liquid velocity is given by

$$u_l + |u_{lw}| = \frac{R^2}{\nu_t}\left[\left(\frac{\tau_w}{2R\rho_l} + \frac{\varepsilon_g g}{2n}\right)(1-\phi^2) - \frac{\varepsilon_g g}{n(n+2)}\left(1-\phi^{n+2}\right)\right] \tag{18}$$

In the above equation, the wall shear stress is related to the velocity at the wall through Eq. (10) as

$$\tau_w = -\rho_l\left(\frac{|u_{lw}|}{11.63}\right)^2 \tag{19}$$

Hence the velocity profile can be calculated if u_{lw} is known. To get an expression for u_{lw}, the mass balance for the liquid phase shown below is used.

$$\int_0^R 2\pi r u_l\left(1-\varepsilon_{gr}\right)dr = -\pi R^2\ |u_{l0}| \tag{20}$$

Using Eq. (18) for the velocity profile and Eq. (15) for the gas holdup profile, the above equation is integrated. This results in a quadratic equation in u_{lw} which when solved gives

$$|u_{lw}| = (11.63)^2\frac{\nu_t J_1}{R}\left[-1 + \sqrt{1 + \frac{\{2J_0-(\varepsilon_g/2)\}}{(11.63)^2 J_1^2}\frac{R^3 g}{\nu_t^2} - \frac{(-2R|u_{l0}|)}{(11.63)^2 J_1(1-\varepsilon_g)\nu_t}}\right] \tag{21}$$

Substituting Eqs. (19) and (21) for τ_w and u_{lw} respectively in Eq. (18), the radial profile of the velocity in terms of known variables is given by

$$u_l = [J_1(1-\phi^2)-1]|u_{lw}| - \frac{R^2 g}{\nu_t}[J_0(1-\phi^2) - I(\phi)] - J_1\left(\frac{|u_{l0}|}{1-\varepsilon_g}\right)(1-\phi^2) \tag{22}$$

The centreline velocity, u_{lc} can be obtained from Eq. (22) by substituting $\phi = 0$,

$$u_{lc} = u_l\Big|_{\phi=0} = \left[J_1-1\right]\left|u_{lw}\right| - \frac{R^2 g}{\nu_t}\left[J_0 - I(\phi=0)\right] - J_1\left(\frac{|u_{l0}|}{1-\varepsilon_g}\right) \tag{23}$$

In Eqs. (21)–(23),

$$J_0 = \frac{\varepsilon_c[(1-\varepsilon_c)(n+2)^2\{(n+2)(n+4-8c)\} + 8\varepsilon_c c\{(n+2)^2 - c(n+4)\}]}{[4(n+2)^2\{(1-\varepsilon_c)(n+2)(n+4) + 8\varepsilon_c c\}]} \tag{24}$$

$$J_1 = \frac{2(n+4)\{(1-\varepsilon_c)(n+2) + 2\varepsilon_c c\}}{(1-\varepsilon_c)(n+2)(n+4) + 8\varepsilon_c c} \tag{25}$$

$$I(\phi) = \varepsilon_c\left\{\frac{1-\phi^2}{4} - \frac{c(1-\phi^{n+2})}{(n+2)^2}\right\} \tag{26}$$

In the above equations, ε_c is the centreline gas holdup related to the average gas holdup by the equation

$$\varepsilon_c = \frac{\varepsilon_g}{\left(1-\frac{2c}{n+2}\right)} \tag{27}$$

The slip velocity in a bubble column represents the difference between the interstitial velocities of the gas and liquid phase. In the homogenous regime, where there are no liquid recirculations, the slip velocity is expressed as

$$u_s = \frac{u_{g0}}{\varepsilon_g} + \frac{|u_{l0}|}{1-\varepsilon_g} \tag{28}$$

However in the heterogeneous regime, due to liquid recirculations, the slip velocity expression gets modified. This modified slip velocity is termed as the apparent slip velocity which can be expressed relating the interstitial gas and liquid velocities as

$$u_s = u_g - u_l \tag{29}$$

An expression for the apparent slip velocity is derived using the gas phase mass balance

$$\int_0^R 2\pi r(u_g)\varepsilon_{gr}dr = \pi R^2 u_{g0} \tag{30}$$

Replacing the interstitial gas phase velocity using Eq. (29) results in,

$$\int_0^R 2\pi r(u_l + u_s)\varepsilon_{gr}dr = \pi R^2 u_{g0} \tag{31}$$

Assuming the apparent slip velocity to be independent of radial position, the above equation is integrated using Eq. (22) for u_l and Eq. (15) for ε_{gr}. In the resulting equation $|u_{lw}|$ is substituted in terms of $u_{lc} + |u_{lw}|$ using Eq. (23). The final equation for the apparent slip velocity is

$$u_s = \frac{u_{g0}}{\varepsilon_g} - \frac{1}{1-\varepsilon_g}\left[-|u_{l0}| + \frac{nc(u_{lc} + |u_{lw}|)}{(n+4)(n+2-2c)}\right] \tag{32}$$

It can be noted that the above equations satisfy the following special cases. Eqs. (21)–(23) and (32) simplify to those (Eqs. (17), (18) and (21) in [17]) given by Ueyama and Miyauchi [17], for the case of zero gas holdup at the wall ($c = 1$). Eqs. (21)–(23) simplify to those given by Kojima et al. [47] for the case of batch liquid ($u_{l0} = 0$).

The liquid velocity radial profile equation (Eq. (22)) can be used to find the radius at which the liquid velocity becomes zero by setting $u_l = 0$. Once this is determined, the average upward liquid velocity in the central core called the mean liquid recirculation velocity can then be calculated using the relation

$$u_{l_{rec}} = \frac{\int_0^{\phi^*}(1-\varepsilon_{gr})u_l\phi d\phi}{\int_0^{\phi^*}(1-\varepsilon_{gr})\phi d\phi} \tag{33}$$

where, ϕ^* is the dimensionless radius at which flow reversal occurs ($u_l = 0$).

4.2.2. Prediction of gas holdup

In this section, application of the above equations to predict the gas holdup measured in countercurrent bubble column is discussed. For a countercurrent bubble column of given diameter, operating at a given gas and liquid velocity and known physical properties of gas and liquid, the above model has two parameters viz. turbulent viscosity and apparent slip velocity. The turbulent viscosity has been correlated in terms of column diameter and gas velocity by Miyauchi et al. [48] using the equation

$$\nu_t = 0.0345 u_{g0}^{\frac{1}{6}} D^{\frac{3}{2}} \tag{34}$$

The same equation is used in the present study also. Based on experimental data on phase velocities, gas holdup, centreline liquid velocity and liquid velocity at wall measured in different bubble columns with batch liquid, Ueyama and Miyauchi [17] showed that the apparent slip velocity increases with gas velocity becoming almost constant at very high gas velocities. However in the case of countercurrent bubble columns, the apparent slip velocity can be a function of both gas and liquid velocities. To determine this dependency, the following steps are followed. Using experimental data on the average gas holdup for given gas and liquid velocities, n and c are calculated using Eqs. (16) and (17) and u_{lw} and u_{lc} are calculated using Eqs. (21) and (23). These values are used in Eq. (32) to get the estimated value of the apparent slip velocity.

The apparent slip velocity is obtained using the experimental data of the present study, Hidaka et al. [11] (u_{l0} up to 10 cm/s) and Besagni and Inzoli [5]. The apparent slip velocity are correlated by the following empirical relation

$$u_s = A u_{g0}^B \exp(C|u_{l0}|); u_s, u_{g0} \text{ and } u_{l0} \text{ in } m/s; 0 < u_{g0} < 0.2;\ 0 < u_{l0} < 0.1 \tag{35}$$

where, $A = 1.57$ (for present study and Hidaka et al. [11]) and 1.35 (for Besagni & Inzoli [5]), $B = 0.44$ and $C = 1.25$. Fig. 12(a) shows the variation of the experimental apparent slip velocity with gas velocity for the three studies along with the values predicted using Eq. (35). The

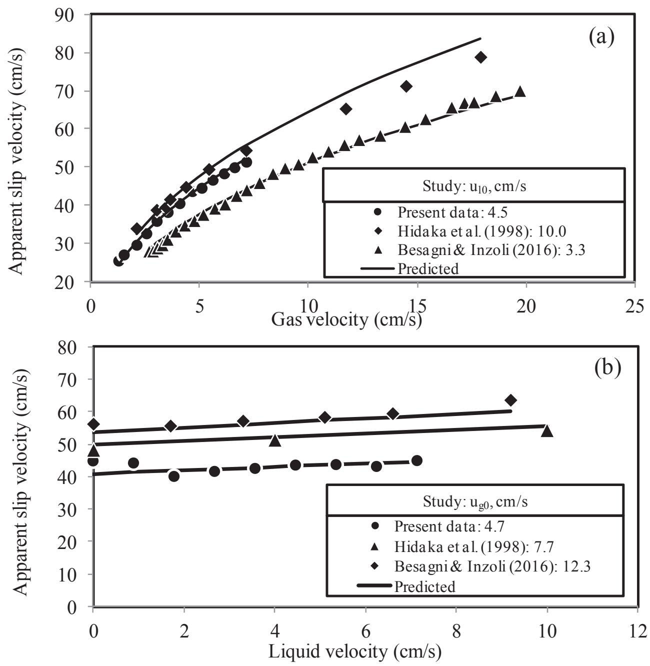

Fig. 12. Variation of apparent slip velocity with (a) gas velocity and (b) liquid velocity.

apparent slip velocity is seen to increase with gas velocity. Such an increasing trend can also be seen from the apparent slip velocity data shown by Ueyama and Miyauchi [17] at low gas velocities. The effect of liquid velocity on the apparent slip velocity is shown in Fig. 12(b). It can be seen that the apparent slip velocity increases with liquid velocity also. It can also be seen from Fig. 12(a) and (b) that Eq. (35) predicts the experimental values satisfactorily including the trend. All the experimental and predicted apparent slip velocities are compared in Fig. 13 with an RMS error of 4.8%.

Using a simplified form of the Ueyama and Miyauchi [17] model (neglecting τ_w and taking $n = 2$ and $c = 1$) and following a procedure similar to that followed in the present work a correlation for apparent slip velocity was obtained by Sekizawa et al. [49]. The correlation is in terms of gas holdup and liquid velocity, thus making it an unknown before predicting the gas holdup. The correlation proposed in the present work has the advantage of showing explicitly the dependence of the apparent slip velocity on gas and liquid velocity and can be calculated apriori. Similar to Sekizawa et al. [48], Hidaka et al. [11] have also used the simplified form of the Ueyama and Miyauchi [17] model and fitted a constant value of turbulent viscosity and apparent slip velocity for their experimental data. The present work uses the detailed Ueyama and Miyauchi [17] model extended for non-zero gas holdup at the wall and allows for generality through correlations for n and c.

Having correlated the apparent slip velocity, for given operating and geometric parameters, Eq. (32) becomes a single non-linear equation in the unknown gas holdup. This non-linear equation is solved using the function 'fsolve' in Matlab. The shear stress term in Eq. (18) and the corresponding terms in Eqs. (21)–(23) have not been neglected while solving for the gas holdup. Though these terms may not be significant at low gas or liquid velocities, but can be significant at high gas or liquid velocities as explained by Wachi et al. [50]. The gas holdup values predicted using the extended Ueyama and Miyauchi [17] model are shown in Fig. 14 for different liquid velocities along with the experimental data measured in the present work. It can be seen that the model predicts the experimental data both qualitatively and quantitatively satisfactorily. However the model over predicts for batch liquid condition due to the relatively large increase in gas holdup with liquid velocity observed experimentally near batch liquid condition. The model also predicts the data of Hidaka et al. [11] and Besagni and Inzoli [5] satisfactorily as seen in Fig. 15(a) and (b). It can be noted that the decreasing effect of liquid velocity on gas holdup at higher gas velocities observed experimentally is also shown by the model. This is especially clear from the predictions for Besagni and Inzoli [5] and Hidaka et al. [11]. The experimental data of the three studies are predicted by the model with an RMS error of 5.2% as shown in Fig. 16.

4.3. Prediction of transition gas velocity and holdup

In Section 4.1, Molerus and Kurtin [35] model has been used to predict the gas holdup in the homogeneous regime as a function of gas and liquid velocities. In Section 4.2, the extended Ueyama and Miyauchi [17] model (Eqs. (16), (17), (21), (23), (32), (34) and (35)) has been used to predict the gas holdup in the heterogeneous regime for different gas and liquid velocities. Hence for a given liquid velocity, the gas holdup can be predicted over the entire range of gas velocities covering both the homogeneous and heterogeneous regimes using respective models. To make the whole modelling process completely predictive, the regime transition velocity should also be predictable. In this way the Molerus and Kurtin [35] model can be applied up to the transition velocity and the extended Ueyama and Miyauchi [17] model above it.

The gas holdup predicted using both the models should be the same at the transition velocity to avoid any discontinuity in the predicted ε_g vs. u_{g0} graph. So for a chosen liquid velocity, both the models were simulated over same range of gas velocities and the gas velocity, at which the difference between the gas holdups is zero, is identified as the transition gas velocity corresponding to that particular liquid velocity. Once the transitional gas velocity is identified, the gas holdup can be obtained from either of the models. This is equivalent to solving both the models simultaneously for transition gas velocity and gas holdup. Such an approach has been used by Sarrafi et al. [51] for a batch bubble column using empirical equations for both the regimes.

The procedure described above is shown graphically in Fig. 17(a) and (b) for the present data for two liquid velocities. The predicted lines using the two models in the respective regions and extended to the other regime for a small range of gas velocities is shown in this figure along with the experimental data. The intersection of the two model lines (shown clearly in the inset) gives the transitional gas velocity and the gas holdup. The solution procedure described above is carried out for different liquid velocities for the present work and Besagni and Inzoli [5]. The transitional gas velocity and gas holdup thus obtained are plotted as a function of liquid velocity along with experimental data in Fig. 18(a) and (b) respectively. It can be seen that the model shows a decrease of transitional gas velocity with liquid velocity in line with the experimental observation. Similarly the model predicts an increase in the gas holdup at transition with liquid velocity similar to the experimental data. The prediction of transitional gas

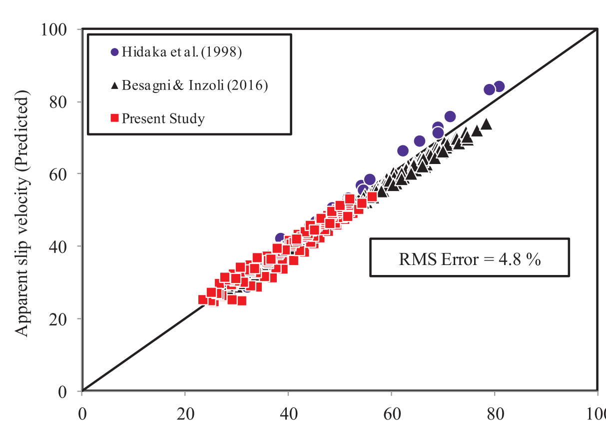

Fig. 13. Comparison of estimated and predicted apparent slip velocity.

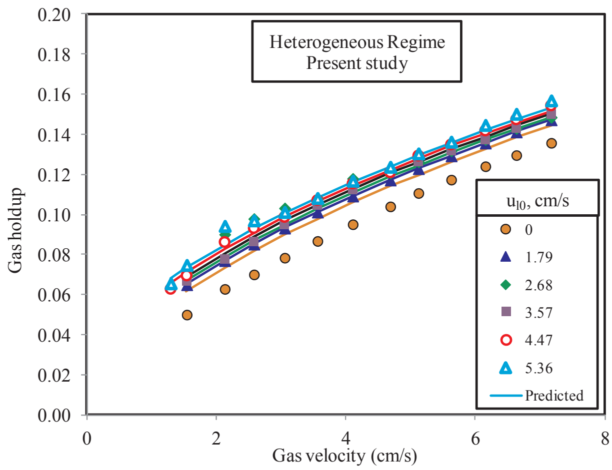

Fig. 14. Prediction of gas holdup in heterogeneous regime using model: effect of phase velocities (Present data).

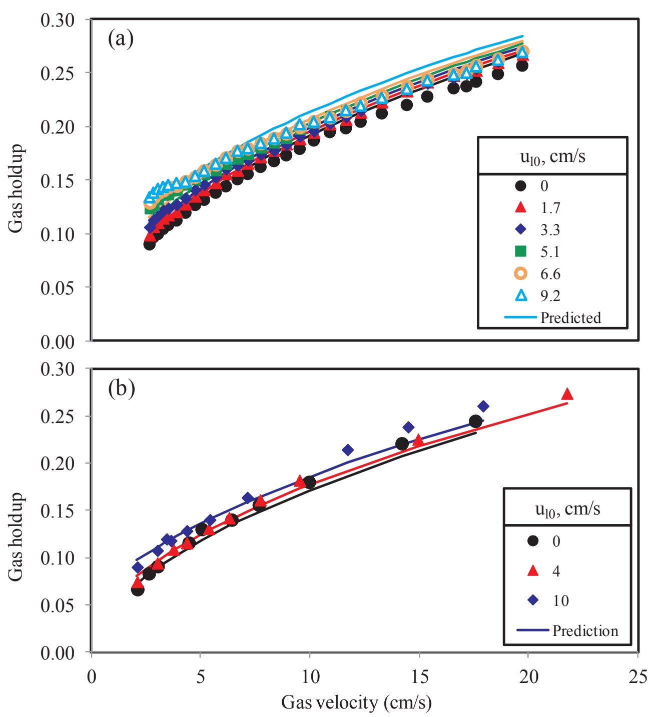

Fig. 15. Prediction of gas holdup using model: effect of phase velocities (a) Besagni and Inzoli (2016) (b) Hidaka et al. (1998).

velocity and gas holdup is satisfactory. To the best of our knowledge, this is the first attempt to predict semi-empirically the effect of liquid velocity on transition gas velocity and holdup in CCBC.

4.4. Simulation of liquid velocity profile

The extended Ueyama and Miyauchi [17] model with the proposed empirical equation for the apparent slip velocity (Eqs. (16) and (17), (21)–(23), (32)–(35)) can be used to simulate the effect of superficial gas and liquid velocities on the radial profile of liquid velocity and the different properties of the radial profile viz. (magnitude of) liquid velocity at wall, centreline liquid velocity, radial position of zero liquid velocity and mean recirculation velocity of the liquid phase in a CCBC. These simulations are carried out for different superficial gas and liquid velocities for the present study, Hidaka et al. [11] and Besagni & Inzoli [5].

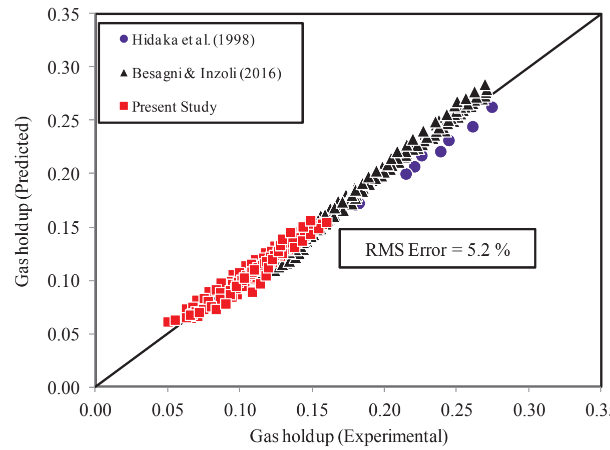

Fig. 16. Comparison of experimental and predicted gas holdup in heterogeneous regime.

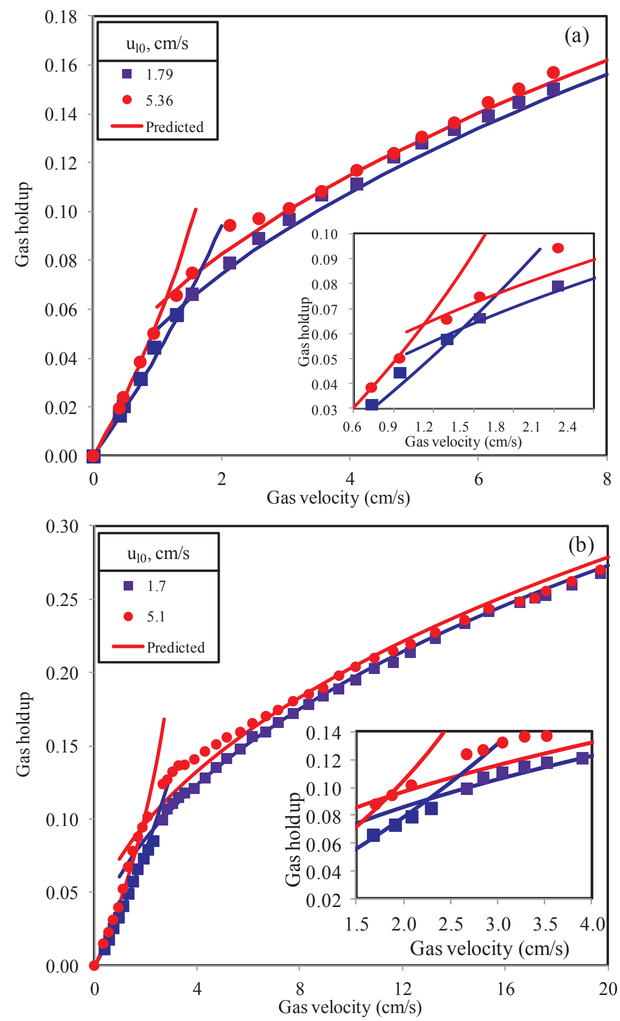

Fig. 17. Determination of regime transition points using model (a) present study (b) Besagni & Inzoli (2016).

The effect of gas and liquid velocity on the radial profile is shown in Fig. 19(a) and (b) respectively. With increase in gas velocity, n decreases according to Eq. (16) making the gas holdup profile and hence the liquid velocity profile steeper. With increase in liquid velocity, since n is taken to be independent of liquid velocity, steepness of the gas holdup profile remains the same and hence the liquid velocity profile shifts almost parallelly down. The effect of gas and liquid velocity on

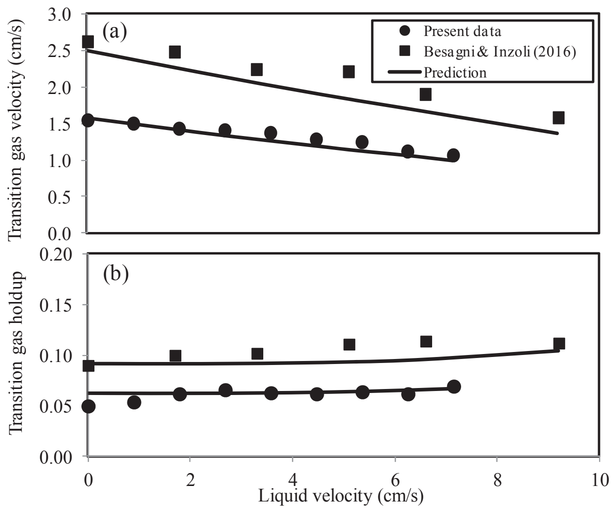

Fig. 18. Prediction of regime transition (a) gas velocity (b) gas holdup using model.

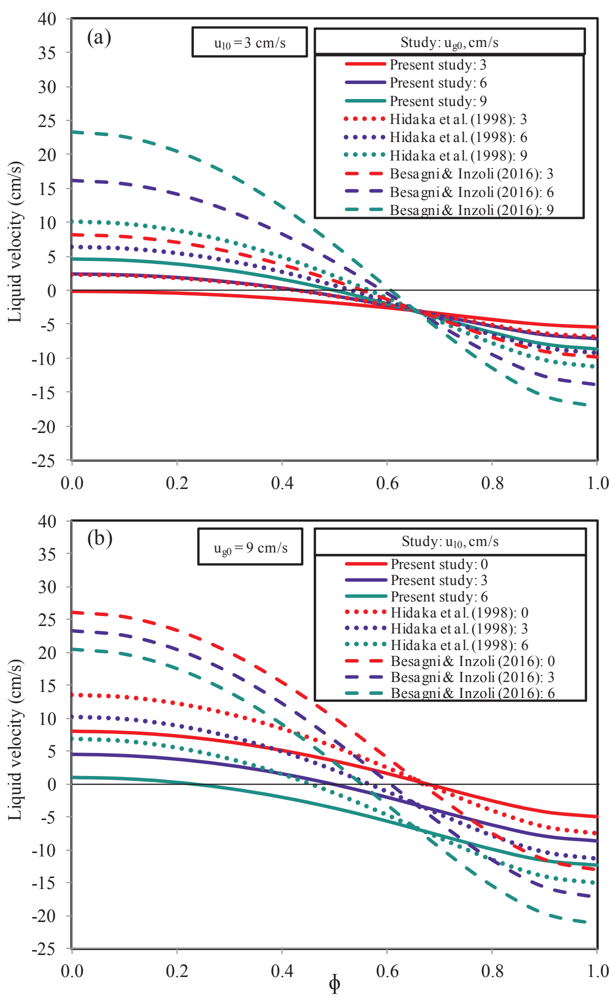

Fig. 19. Effect of (a) gas and (b) liquid velocity on radial profile of liquid velocity.

the properties of the radial profile is shown in Figs. 20 and 21 respectively. Figs. 20(a) and 21(a) show the variation of velocity at wall with superficial gas and liquid velocity respectively for the three studies. The velocity at wall increases with both gas and liquid velocities. At constant liquid velocities, with increase in gas velocity, liquid recirculations increase and hence to satisfy the liquid phase mass balance the velocity at the wall increases. At a constant gas velocity, with increase in liquid velocity the liquid circulation is suppressed due to countercurrent flow. However because of the dominating effect of increase in liquid velocity, the velocity at the wall increases.

The variation of centreline velocity with gas and liquid velocity is shown in Figs. 20(b) and 21(b) respectively. With increased gas velocity, liquid recirculations increase resulting in higher centreline velocity. With increase in liquid velocity, the centreline velocity decreases due to the countercurrent direction of liquid flow. It can be seen that the centreline velocity decreases to values lower than zero (negative values in Figs. 20(b) and 21(b) indicate liquid flowing down in the centre of the column) beyond a particular liquid velocity for the present study. Under such conditions the velocity is in the downward direction throughout the entire cross-section. The liquid velocity at which the centreline velocity becomes zero increases with gas velocity due to higher liquid circulations.

Figs. 20(c) and 21(c) shows the effect of the phase velocities on the (dimensionless) radial position (ϕ^*) at which the liquid velocity becomes zero. With increase in gas velocity, this radial position moves towards the wall since the liquid velocity profile becomes steeper. The shifting effect increases with increase in liquid velocity. With increase in liquid velocity, this radial position moves towards the centre of the column since the liquid velocity profile shifts almost parallelly down. The shift is steeper at low gas velocities. Beyond a certain liquid velocity, as discussed above, the velocity is negative throughout the cross-section and ϕ^* has no meaning beyond this liquid velocity. Hence the lines in Figs. 20(c) and 21(c) are shown till these liquid velocities only corresponding to the different gas velocities.

The variation of the mean liquid recirculation velocity with the phase velocities is shown in Figs. 20(d) and 21(d). Similar to the centreline velocity, the mean liquid recirculation velocity increases with gas and decreases with liquid velocities. Beyond the liquid velocity at which the local liquid velocity is negative throughout the column, liquid circulation velocity is not applicable and hence not shown in the figure.

5. Conclusions

In the present work, hydrodynamic studies have been carried out in CCBC using a porous plate gas distributor. Porous plates have been used because they generate smaller bubbles that increase mass transfer rates. Using the swarm velocity method, four flow regimes have been identified. These regimes in the order of increasing gas velocity are: purely homogeneous bubbling regime, discrete bubbling regime, helical flow regime and churn-turbulent regime. Flow regime map showing the effect of liquid velocity on the gas velocity for regime transition has been developed. This reveals that the transition from purely homogeneous bubbling regime to discrete bubbling regime, discrete bubbling regime to helical flow regime and helical flow regime to churn-turbulent regime all advances with increase in liquid velocity. This can be explained based on the variation of gas holdup along the regime boundaries, which increases with liquid velocity along all the three regime boundaries. Similar to the bubble column with batch liquid, in the CCBC also, the gas holdup increases with gas velocity in all the four regimes with a slower rate in the heterogeneous regime. Increase in liquid velocity causes a local maximum in the gas holdup-gas velocity plot similar to the effect of small orifice diameters and surface active agents in semi-batch bubble columns. In the CCBC, the gas holdup is found to increase with increase in liquid velocity since the countercurrent flow increases the residence time of the bubbles.

The hydrodynamics of the CCBC has been predicted semi-empirically by combining two phenomenological models. The model proposed by Molerus and Kurtin [35] is used for the homogeneous regime with the bubble diameter as the parameter. The bubble diameter is found to decrease with increase in liquid velocity probably due to increased liquid phase turbulence. The recirculation model proposed by Ueyama and Miyauchi [17] has been extended to predict the gas holdup in

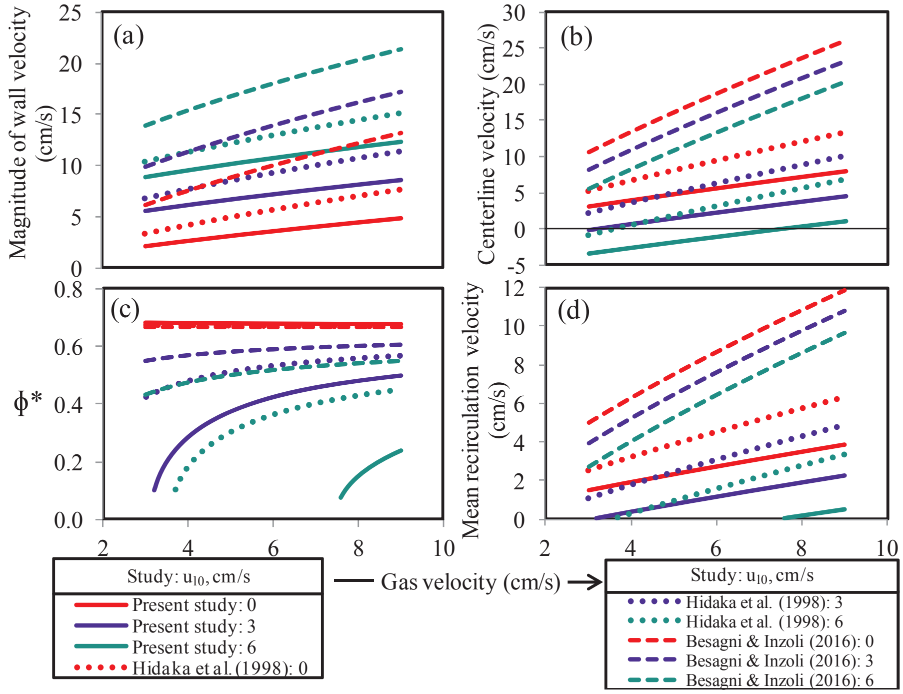

Fig. 20. Effect of gas velocity on (a) magnitude of velocity at wall (b) centreline velocity (c) dimensionless flow reversal radius (d) mean recirculation velocity.

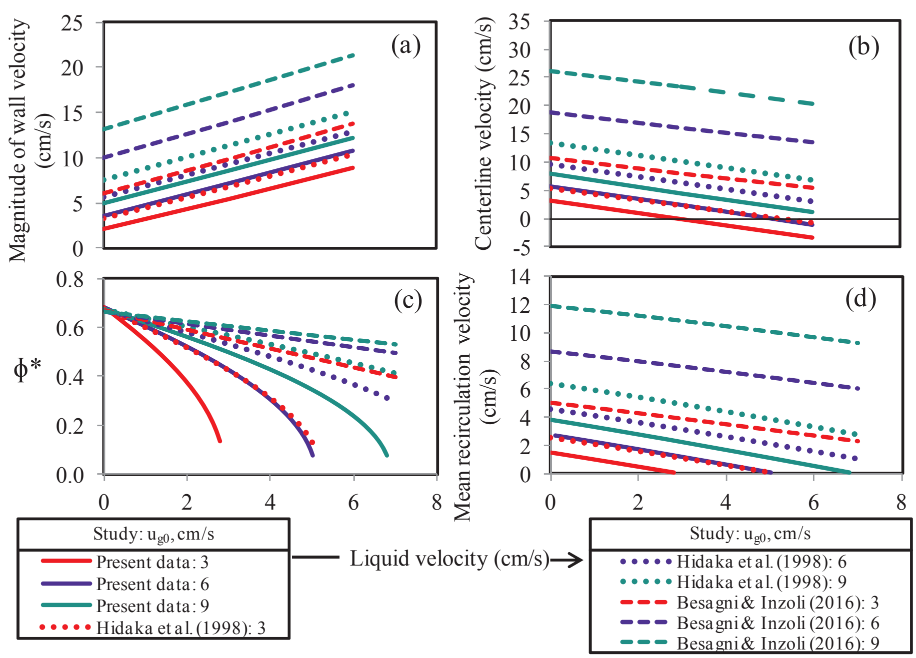

Fig. 21. Effect of liquid velocity on (a) magnitude of velocity at wall (b) centreline velocity (c) dimensionless flow reversal radius (d) mean recirculation velocity.

heterogeneous regime with apparent slip velocity as the parameter. The apparent slip velocity increases with both gas and liquid phase velocities. The transition velocity between the homogeneous and heterogeneous regime is also predicted by the simultaneous solution of both the models. The proposed method satisfactorily predicts the data on gas holdup, transition gas velocity and holdup at transition, from the present study and literature.

Based on the proposed correlation for apparent slip velocity, the effect of gas and liquid velocity on the radial profile of liquid velocity and its properties is simulated. The (magnitude of) velocity at wall, centreline velocity, radius of flow reversal and mean recirculation velocity increases with gas velocity. Apart from the velocity at wall, all the properties decrease with liquid velocity. The method developed in the present work is valuable as it is (i) comprehensive in predicting gas holdup in both the regimes and the transition velocities and (ii) generic in being able to predict the hydrodynamics over a wide range of gas and liquid velocities.

References

[1] C. Leonard, J.-H. Ferrasse, O. Boutin, S. Lefevre, A. Viand, Bubble column reactors for high pressures and high temperatures operation, Chem. Eng. Res. Des. 100 (2015) 391–421.
[2] T.A. Bartrand, B. Farouk, C.N. Haas, Countercurrent gas/liquid flow and mixing: Implications for water disinfection, Int. J. Multiphase Flow 35 (2009) 171–184.
[3] T. Renganathan, K. Krishnaiah, Prediction of minimum fluidization velocity in two and three phase inverse fluidized beds, Can. J. Chem. Eng. 81 (2003) 853–860.
[4] T. Renganathan, K. Krishnaiah, Voidage characteristics and prediction of bed expansion in liquid-solid inverse fluidized bed, Chem. Eng. Sci. 60 (2005) 2545–2555.
[5] G. Besagni, F. Inzoli, Comprehensive experimental investigation of counter-current

bubble column hydrodynamics: Holdup, flow regime transition, bubble size distributions and local flow properties, Chem. Eng. Sci. 146 (2016) 259–290.
[6] G. Besagni, A. Di Pasquali, L. Gallazzini, E. Gottardi, L.P.M. Colombo, F. Inzoli, The effect of aspect ratio in counter-current gas-liquid bubble columns: experimental results and gas holdup correlations, Int. J. Multiph. Flow 94 (2017) 53–78.
[7] T. Otake, S. Tone, K. Shinohara, Gas holdup in the bubble column with cocurrent and countercurrent gas-liquid flow, J. Chem. Eng. Jpn 14 (1981) 338–340.
[8] S. Uchida, S. Tsuyutani, T. Seno, Flow regimes and mass transfer in counter-current bubble columns, Can. J. Chem. Eng. 67 (1989) 866–869.
[9] T. Seno, S. Uchida, S. Tsuyutani, Mass transfer in countercurrent and cocurrent bubble columns, Chem. Eng. Technol. 13 (1990) 113–118.
[10] M. Roustan, R.Y. Wang, Wolbert, Modeling hydrodynamics and mass transfer parameters in a continuous ozone bubble column, Ozone Sci. Eng. 18 (1996) 99–115.
[11] N. Hidaka, K.I. Mizuguchi, T. Matsumoto, Axial mixing of liquid in counter-current bubble columns, J. Chem. Eng. Jpn. 31 (1998) 1016–1019.
[12] H. Jin, S. Yang, G. He, M. Wang, R.A. Williams, The effect of gas-liquid countercurrent operation on gas hold-up in bubble columns using electrical resistance tomography, J. Chem. Technol. Biotechnol. 85 (2010) 1278–1283.
[13] F. Hernandez-Alvarado, D.V. Kalaga, S. Banerjee, M. Kawaji, Comparison of Gas Hold-up Profiles in Co-current, Counter-current and Batch Bubble Column Reactors Measured Using Gamma Densitometry and Surface of Revolution Method, ASME, Fluids Engineering Division (Publication) FEDSM, Washington, DC, USA, 2016.
[14] M. Shah, A.A. Kiss, E. Zondervan, J. Van der Schaaf, A.B. De Haan, Gas holdup, axial dispersion, and mass transfer studies in bubble columns, Ind. Eng. Chem. Res. 51 (2012) 14268–14278.
[15] A.K. Biń, B. Duczmal, P. Machniewski, Hydrodynamics and ozone mass transfer in a tall bubble column, Chem. Eng. Sci. 56 (2001) 6233–6240.
[16] S.M. Son, P.S. Song, C.G. Lee, S.H. Kang, Y. Kang, K. Kusakabe, Bubbling behavior in gas–liquid countercurrent bubble column bioreactors, J. Chem. Eng. Jpn 37 (2004) 990–998.
[17] K. Ueyama, T. Miyauchi, Properties of recirculating turbulent two phase flow in gas bubble columns, AIChE J. 25 (1979) 258–266.
[18] A. Shaikh, M.H. Al-Dahhan, A review on flow regime transition in bubble columns, Int. J. Chem. React. Eng. 5 (2007).
[19] N. Zuber, J.A. Findlay, Average volumetric concentration in two-phase flow systems, J. Heat Transfer 87 (1965) 453–468.
[20] G.B. Wallis, One-dimensional Two-phase Flow, McGraw-Hill, New York, 1969.
[21] M.C. Ruzicka, J. Zahradník, J. Drahoš, N.H. Thomas, Homogeneous-heterogeneous regime transition in bubble columns, Chem. Eng. Sci. 56 (2001) 4609–4626.
[22] M.T. Ityokumbul, N. Kosaric, W. Bulani, Gas hold-up and liquid mixing at low and intermediate gas velocities. I. Air-water system, Chem. Eng. J. Biochem. Eng. J. 53 (1994) 167–172.
[23] R.C. Chen, J. Reese, L.S. Fan, Flow structure in a three-dimensional bubble column and three-phase fluidized bed, AIChE J. 40 (1994) 1093–1104.
[24] Z. Cui, Hydrodynamics in a Bubble Column at Elevated Pressures and Turbulence Energy Distribution in Bubbling Gas-liquid and Gas-liquid-solid Flow Systems (Ph.D. Thesis), Ohio State University, Ohio, 2005.
[25] S. Nedeltchev, New methods for flow regime identification in bubble columns and fluidized beds, Chem. Eng. Sci. 137 (2015) 436–446.
[26] R. Krishna, P.M. Wilkinson, L.L. Van Dierendonck, A model for gas holdup in bubble columns incorporating the influence of gas density on flow regime transitions, Chem. Eng. Sci. 46 (1991) 2491–2496.
[27] C. Hyndman, F. Larachi, C. Guy, Understanding gas-phase hydrodyamics in bubble columns: a convective model based on kinetic theory, Chem. Eng. Sci. 52 (1997) 63–77.
[28] B. Gourich, C. Vial, A.H. Essadki, F. Allam, M.B. Soulami, M. Ziyad, Identification of flow regimes and transition points in a bubble column through analysis of differential pressure signal – influence of the coalescence behavior of the liquid phase, Chem. Eng. Proc. 45 (2006) 214–223.
[29] C.P. Ribeiro, D. Mewes, The influence of electrolytes on gas hold-up and regime transition in bubble columns, Chem. Eng. Sci. 62 (2007) 4501–4509.
[30] H.M. Letzel, J.C. Schouten, C.M. Van den Bleek, R. Krishna, Influence of elevated pressure on the stability of bubbly flows, Chem. Eng. Sci. 52 (1997) 3733–3739.
[31] S.H. Eissa, K. Schügerl, Holdup and backmixing investigations in cocurrent and countercurrent bubble columns, Chem. Eng. Sci. 30 (1975) 1251–1256.
[32] J. Zahradník, M. Fialová, M. Růžička, J. Drahoš, F. Kaštánek, N.H. Thomas, Duality of the gas-liquid flow regimes in bubble column reactors, Chem. Eng. Sci. 52 (1997) 3811–3826.
[33] J.F. Richardson, W.N. Zaki, The sedimentation of a suspension of uniform spheres under conditions of viscous flow, Chem. Eng. Sci. 3 (1954) 65–73.
[34] C. Garnier, M. Lance, J.L. Maria, Measurement of local flow characteristics in buoyancy-driven bubbly flow at high void fraction, Exp. Therm. Fluid Sci. 26 (2002) 811–815.
[35] O. Moleurs, M. Kurtin, Hydrodynamics of bubble columns in the uniform bubbling regime, Chem. Eng. Sci. 40 (1985) 647–652.
[36] S. Nedeltchev, A. Schumpe, A new approach for the prediction of gas holdup in bubble columns operated under various pressures in the homogeneous regime, J. Chem. Eng. Jpn 41 (2008) 744–755.
[37] P.M. Wilkinson, H. Haringa, L.L. Van Dierendonck, Mass transfer and bubble size in a bubble column under pressure, Chem. Eng. Sci. 49 (1994) 1417–1427.
[38] O. Molerus, A coherent representation of pressure drop in fixed beds and of bed expansion for particulate fluidized beds, Chem. Eng. Sci. 35 (1980) 1331–1340.
[39] O. Molerus, Principles of Flow in Disperse Systems, Chapman and Hall, London, 1993.
[40] T. Takahashi, T. Miyahara, S. Senzai, H. Terakado, Bubble formation at submerged nozzles in cocurrent, countercurrent and crosscurrent flow, Kagaku Kogaku Ronbunshu 6 (1980) 563–568.
[41] J.B. Joshi, Computational flow modelling and design of bubble column reactors, Chem. Eng. Sci. 56 (2001) 5893–5933.
[42] J.B. Joshi, U.P. Veera, C.V. Prasad, D.V. Phanikumar, Gas hold-up structure in bubble column reactors, PINSA 64A (4) (1998) 441–567.
[43] Y. Kato, M. Nishinaka, S. Morooka, Distribution of gas holdup in a bubble column, Kagaku Kogaku Ronbunshu 1 (1975) 530–533.
[44] H. Luo, H.F. Svendsen, Turbulent circulation in bubble columns from eddy viscosity distributions of single-phase pipe flow, Can. J. Chem. Eng. 69 (1991) 1389–1394.
[45] L.F. Burns, R.G. Rice, Circulation in bubble columns, AIChE J. 43 (1997) 1390–1402.
[46] Y. Wu, B. Cheng Ong, M.H. Al-Dahhan, Predictions of radial gas holdup profiles in bubble column reactors, Chem. Eng. Sci. 56 (2001) 1207–1210.
[47] E. Kojima, H. Unno, Y. Sato, T. Chida, Liquid phase velocity in a 5.5 M diameter bubble column, J. Chem. Eng. Jpn. 3 (1980) 16–21.
[48] T. Miyauchi, S. Furusaki, S. Morooka, Y. Ikeda, Transport phenomena and reaction in fluidized catalyst beds, Adv. Chem. Eng. 11 (1981) 275–448.
[49] T. Sekizawa, H. Kubota, W.C. Chung, Apparent slip velocity with recirculating turbulent flow in bubble columns, J. Chem. Eng. Jpn 16 (1983) 327–330.
[50] S. Wachi, H. Morikawa, K. Ueyama, Gas holdup and axial dispersion in gas-liquid concurrent bubble column, J. Chem. Eng. Jpn 20 (1987) 309–316.
[51] A. Sarrafi, M. Jamialahmadi, H. Müller-Steinhagen, J.M. Smith, Gas holdup in homogeneous and heterogeneous gas—liquid bubble column reactors, Can. J. Chem. Eng. 77 (1999) 11–21.
[52] J. Todt, J. Lücke, K. Schügerl, A. Renken, Gas holdup and longitudinal dispersion in different types of multiphase reactors and their possible application for microbial processes, Chem. Eng. Sci. 32 (1977) 369–375.